

A numerical study of ionospheric profiles for mid-latitudes

Shun-Rong Zhang, Xin-Yu Huang

Wuhan Ionospheric Observatory, Wuhan Institute of Physics, Chinese Academy of Sciences, P.O. Box 71010, 430071, Wuhan, P.R. China

Received 18 May 1994/Revised 28 July 1994/Accepted 26 August 1994

Abstract. This paper presents a numerical model and results for the mid-latitude ionospheric profile below the peak of the F_2 -layer. The basis of the model is the solving of equations for four ionic species O^+ , NO^+ , O_2^+ and N_2^+ , as well as the meta-stable $O^+(^2D)$ and $O^+(^2P)$. Diffusion and wind-induced drifts and 21 photo-chemical reactions are also taken into account. Neutral atmospheric density and temperature are derived from the MSIS86 model and solar extreme ultraviolet irradiance from the EUV91 model. In an effort to obtain a more realistic ionospheric profile, the key point at foF_2 and hmF_2 is fitted from the simulation to observations. The model also utilizes the vertical drifts derived from ionosonde data with the help of the Servo model. It is shown that the ionospheric height of peak can be reproduced more accurately under the derived vertical drifts from the Servo theory than with the HWM90 model. Results from the simulation are given for Wuchang (30.5°N, 114.4°E) and Wakkanai (45.6°N, 141.7°E), showing the profile changes with season and solar activity, and the E–F valley structure (the depth and the width). This simulation also reveals the importance of meta-stable ions and dynamical transport processes on the formation of the F_1 -ledge and F_1 – F_2 valley.

1 Introduction

Ionospheric electron and ion density profiles can be extracted from ionosonde and incoherent scatter radar observational data. Difficulties arise from the original data analysis for some particular ionospheric regions. On the ionograms, the no-echo phenomenon can be constantly observed between the E- and F-layers, and in some cases, for example, near noon in the summer of lower solar activity over Wuchang (30.5°N, 114.4°E), the phenom-

enon can also appear between the F_1 – F_2 -layer (Huang and Li, 1992). The presentation of these no-echo phenomena implies in great measure the occurrence of the valley. It is then difficult to gain realistic information in the valley, as well as above the valley. Radars cannot distinguish between NO^+ and O_2^+ , and it is difficult to simultaneously determine the ion composition and the ion temperature. These problems have partly led to the relatively poor understanding of the ionospheric structure as a whole, compared with other ionospheric characteristics which have been well defined. The related profile prediction of electrons and ions to an acceptable level of accuracy seems unrealistic at present.

Numerical simulation of theoretical ionospheric profiles may be one possible solution to this problem, if it can be carried out in such a way that not only a general understanding of the physical and chemical processes is necessary, but also a detailed pattern of the profile is pursued. The product of this research will at least provide a reference for profile inversion, especially regarding the valley and the surrounding area. This requires a more appropriate determination of background parameters as well as the major processes. Generally, a theoretical profile which is obtained numerically by solving the equations of continuity, momentum and sometimes energy for ionic species, with neutral density and wind, etc. as inputs, cannot exactly correlate with those observed, mainly due to incorrect inputs. In the E- and low F-regions, where chemical processes dominate, neutral density and EUV flux are especially important, whilst in the F_2 -region, additional considerations must be made for neutral wind, diffusion and electric field. In this context, the current modeling work needs to be improved, so that a full ionospheric profile can be achieved with practical application.

This paper attempts to study numerically the mid-latitude ionospheric profile in which the key point, at the F_2 peak, is fitted to observed ionosonde data. The deduced height of the peak hmF_2 (hereafter “observed peak height” or “observed hmF_2 ”) from $M3000F_2$ (Dudeney, 1983) may be obtained in the simulated profile, using vertical drifts

derived from the Servo model (Rishbeth *et al.*, 1978). The Servo model suffers from a shortcoming arising from the assumption of equilibrium in the ionosphere, which is believed by Titheridge (1993) to be unrealistic in the period between sunrise and pre-noon. However, the present study indicates that the derived peak height can generally be accurately reproduced even for 07–14 LT if the Servo-model-based drift is used. The theoretical model presented here also adopts the recent EUV91 flux model (Tobiska, 1991).

The aim of this paper is to establish a numerical model that can be used to study the time-dependent ionospheric profile at mid-latitudes and to give preliminary results for the simulation. Following a detailed description of the model in Sect. 2, we consider in Sect. 3 the ionospheric F_2 peak response to HMM90 winds (Hedin *et al.*, 1991) and Servo-model-based vertical drifts, the F_1 -ledge related phenomena and the E–F valley structure. Section 4 contains a summary of this investigation.

2 Model

A one-dimensional and time-dependent ionospheric model is employed in this study, based on the previous work of Zhang *et al.* (1993, hereafter Paper I). The model

includes 21 chemical reactions (shown in Tables 1 and 2), for four ionic species, i.e. O^+ , NO^+ , O_2^+ and N_2^+ , as well as the meta-stable $O^+(^2D)$ and $O^+(^2P)$ besides the stable $O^+(^4S)$ (denoted as O^+ in Table 1 for simplification). The solar extreme ultraviolet flux term is based on the recent model EUV91 which introduces the day-to-day variability of the flux. Therefore, varying from Paper I, the present model allows for reactions of meta-stable ions and adopts the new EUV model; some of the reaction rates are also revised. The scheme of chemical reactions is similar to the Buonsanto model (1990) and Buonsanto *et al.* (1992) in respect of the eight reactions for stable ions, whilst the present model contains more meta-stable reactions, including, in particular, the branching of the $O^+(^2D) + N_2$ reaction to N_2^+ and $O^+(^4S)$. This branching, even with the reaction rates still not well-defined, seems important for the ionospheric F_1 -region. Here we take the reaction rates for branching as $10^{-10} \text{ cm}^{-3} \text{ s}^{-1}$ (see Torr and Torr, 1982). Varying from Buonsanto (1990) and Buonsanto *et al.* (1992), the present model makes no modification to the outputs of the EUV91 model and the neutral atmospheric model MSIS86 (Hedin, 1987).

As for the dynamical scheme, the effects of diffusion and wind on the atomic and the molecular ions are treated individually. The transport term in the continuity equations with regard to molecular ions is primarily ignored

Table 1. Chemical reactions and rates for stable ions

$O^+ + N_2 \rightarrow NO^+ + N$	$(k_1 = 1.533 \times 10^{-12} - 5.92 \times 10^{-13} (T/300) + 8.60 \times 10^{-14} (T/300)^2)$	(1)
$O^+ + O_2 \rightarrow O_2^+ + O$	$(k_2 = 2.82 \times 10^{-11} - 7.74 \times 10^{-12} (T/300) + 1.073 \times 10^{-12} (T/300)^2 - 5.17 \times 10^{-14} (T/300)^3 + 9.65 \times 10^{-16} (T/300)^4)$	(1)
$O_2^+ + NO \rightarrow NO^+ + O_2$	$(k_3 = 4.4 \times 10^{-10})$	(2)
$O_2^+ + e \rightarrow O + O$	$(k_4 = 2.0 \times 10^{-7} (300/T_e)^{0.7})$	(3)
$N_2^+ + O_2 \rightarrow O_2^+ + N_2$	$(k_5 = 5.0 \times 10^{-11} (300/T))$	(2)
$N_2^+ + O \rightarrow NO^+ + N$	$(k_6 = 1.4 \times 10^{-10} (300/T)^{0.44})$	(4)
$N_2^+ + e \rightarrow N + N$	$(k_7 = 1.8 \times 10^{-7} (300/T_e)^{0.39})$	(5)
$NO^+ + e \rightarrow N + O$	$(k_8 = 4.2 \times 10^{-7} (300/T_e)^{0.85})$	(6)

All the rates are in $\text{cm}^3 \text{ s}^{-1}$. (1) St. Maurice and Torr (1978); (2) Lindinger *et al.* (1974); (3) Walls and Dunn (1974); (4) McFarland *et al.* (1974); (5) Mehr and Biondi (1969); (6) Torr *et al.* (1976)

Table 2. Chemical reactions and rates for meta-stable ions

$O^+(^2D) + N_2 \rightarrow N_2^+ + O$	$(\alpha_1 = 10^{-10})$	(7)
$O^+(^2D) + O_2 \rightarrow O_2^+ + O$	$(\alpha_2 = 7 \times 10^{-11})$	(8)
$O^+(^2D) + O \rightarrow O^+(^4S) + O$	$(\alpha_3 = 10^{-11})$	(9)
$O^+(^2D) + e \rightarrow O^+(^4S) + e$	$(\alpha_4 = 7.8 \times 10^{-8} (T_e/300)^{-1/2})$	(7)
$O^+(^2D) \rightarrow O^+(^4S) + h\nu$	$(A_1 = 7.7 \times 10^{-5} \text{ s}^{-1})$	(7)
$O^+(^2D) + N_2 \rightarrow O^+(^4S) + N_2$	$(\alpha_5 = 1 \times 10^{-10})$	(10)
$O^+(^2P) + N_2 \rightarrow N_2^+ + O$	$(\gamma_1 = 4.8 \times 10^{-10})^a$	(11)
$O^+(^2P) + N_2 \rightarrow N^+ + NO$	$(\gamma_2 = 1 \times 10^{-11})$	(7)
$O^+(^2P) + O \rightarrow O^+(^4S) + O$	$(\gamma_3 = 5.2 \times 10^{-11})^a$	(11)
$O^+(^2P) + e \rightarrow O^+(^4S) + e$	$(\gamma_4 = 4.0 \times 10^{-8} (T_e/300)^{-1/2})$	(7)
$O^+(^2P) + e \rightarrow O^+(^2D) + e$	$(\gamma_5 = 1.5 \times 10^{-7} (T_e/300)^{-1/2})$	(12)
$O^+(^2P) \rightarrow O^+(^4S) + h\nu$	$(B_1 = 0.047 \text{ s}^{-1})$	(13)
$O^+(^2P) \rightarrow O^+(^2D) + h\nu$	$(B_2 = 0.171 \text{ s}^{-1})$	(13)

All the rates are in $\text{cm}^3 \text{ s}^{-1}$, except A_1 , B_1 , B_2 in s^{-1} .

^a Coefficient should be enhanced by 15–30% (cf. Torr and Torr, 1982) (7) Rees (1989); (8) Johnsen and Biondi (1980); (9) Torr and Torr (1980); (10) Torr and Torr (1982); (11) Rusch *et al.* (1977); (12) Henry *et al.* 1969 (13) Seaton and Osterbrock (1957)

for reducing the computing time, except when we focus on the F_1 -ledge and F_1 - F_2 -valley-related processes. In these cases, the model includes molecular ions transports induced by neutral winds and their diffusions are assumed to be ignorable. For O^+ , we combine the continuity and the momentum equation with diffusion and wind always considered, as in Paper I. The model is valid at mid-latitudes within the range of 100–500 km, as we consider only the vertical transport and ignore the H^+ contribution. The time and height intervals are 15 min and 2 km, respectively.

The peak of the F_2 -layer is a key point on the profile and should be fitted to observations, so that the simulated profiles have more practical meaning. This action overcomes two problems that have commonly arisen in similar models. The first problem concerns the choice of topside values for solving the diffusion equation of O^+ . These values can be taken from IRI (Bilitza, 1990), however test calculations indicate that increasing O^+ density by 10% for the whole 24 h will result in a corresponding decrease of around 5% in the maximum electron density. Therefore, a more realistic topside density is necessary and this can be achieved by adjusting the initial topside values (e.g. IRI values), so that the simulated foF_2 can be fitted to that observed. In other words, the observed foF_2 values may be utilized as input in this model. It should also be pointed out that adjustment of the topside O^+ density implies a modification in the topside flux, and this modification will result in a change of hmF_2 (Sica *et al.*, 1990; Kirchengast *et al.*, 1992). Our test calculation indicates that a 50% change of topside density causes an hmF_2 shift of no more than 6 km in the daytime and almost no shift at night-time. With regard to the precision with which hmF_2 can be derived from the $M3000F_2$ factor, we may assume that the shift due to topside density (flux) change, although physically meaningful, can be ignored in the present study. The second problem experienced by the previous models is that the background meridional wind acts efficiently to modify the ionospheric F_2 -layer behavior, especially the ionization height. This means that the peak height can be reproduced only if an appropriate meridional wind is used.

Servo model calculations provide a quick method to derive vertical drifts induced by neutral wind and $\mathbf{E} \times \mathbf{B}$, by using ionospheric F_2 -layer parameters foF_2 and hmF_2 . Several results have been obtained for different research purposes (e.g. Buonsanto *et al.*, 1989). However, Titheridge (1993) pointed out that, the assumption of equilibrium ionosphere might not be valid, especially in the period between sunrise and pre-noon since his model study showed obvious differences between the Servo-model-based balance height and the peak height with neutral wind not applied in his theoretical model. It is not clear at present whether this off-equilibrium behavior causes significant errors. As will be shown below, simulated peak heights, when Servo-model-based vertical drifts are used, are generally in agreement with the observed height. This agreement suggests that the simple theory of the Servo model can provide the true vertical drifts, with which more complex theoretical calculations can then accurately reproduce the observed peak heights.

The method used here to derive drifts is similar to the work of Buonsanto *et al.* (1989), in which foF_2 and hmF_2 must be used. It should be noted that Servo model calculations give the drift near the F_2 peak. In the present study, the same function as that in the HWM90 model is used to represent the height variation for the drift.

In summary, the model may fix the simulated maximum electron density of the ionosphere with the observed NmF_2 through modification of the initial topside values. The observed hmF_2 may also be used, in accordance with the Servo theory, so that an equivalent component of the background wind-induced (and probably electromagnetic) drift can be more precisely determined. With such drift the hmF_2 can be accurately reproduced in return by the present model. Finally, it should be mentioned that our current model does not account for electric field, as we assume it is not an important factor over the Wakkanai station (45.6°N, 141.7°E). When the derived equivalent drift is used, it is necessary to disregard the electric field.

3 Results and discussions

3.1 Ionospheric height of peak

Simulations are conducted using in turn the different background wind/drift, i.e. HWM90 winds and Servo-model-based drifts and different topside values, i.e. the IRI90 and that modified to fit the observed foF_2 . Figure 1 shows some results for the peak height. At Wakkanai, HWM90 wind (with topside values determined by the IRI) gives a higher altitude of the peak hmF_2 at night-time and a slightly lower hmF_2 in the daytime than that observed, probably indicating that the night-time southward meridional wind and the daytime northward component are too strong. This supports the prior conclusion that the HWM90 model overestimates the equatorward component in the F_2 -region (see Kirchengast *et al.*, 1992, and references therein). The disagreement is more serious in equinox months (March and September). However, when derived vertical drifts are introduced according to the Servo model, very good agreement between the simulated and the observed hmF_2 can be found for the 4 months at this station (even for 07–14LT). Generally, the hmF_2 departure is less than 20 km, which is smaller than that of around 50 km at night-time when the HWM90 is used. These are the cases when IRI topside values are used in the two different wind/drift calculations.

Using observed foF_2 to adjust the initial topside values, the simulated hmF_2 still approaches that observed for Wakkanai (not shown here). Again, the situation is better when Servo-model-based drifts rather than HWM90 winds are employed. For Wuchang (30.5°N, 114.4°E) which has a lower latitude than Wakkanai, a similar conclusion for the HWM90 and derived drifts can be obtained (Fig. 2). However, it can also be seen from Fig. 2 that some “jumps” and “noise” exist on the hmF_2 diurnal curves. As mentioned earlier, the adjustment of topside density (flux) can lead to hmF_2 change. Thus, when the observed foF_2 (monthly medians) undergoes an obvious

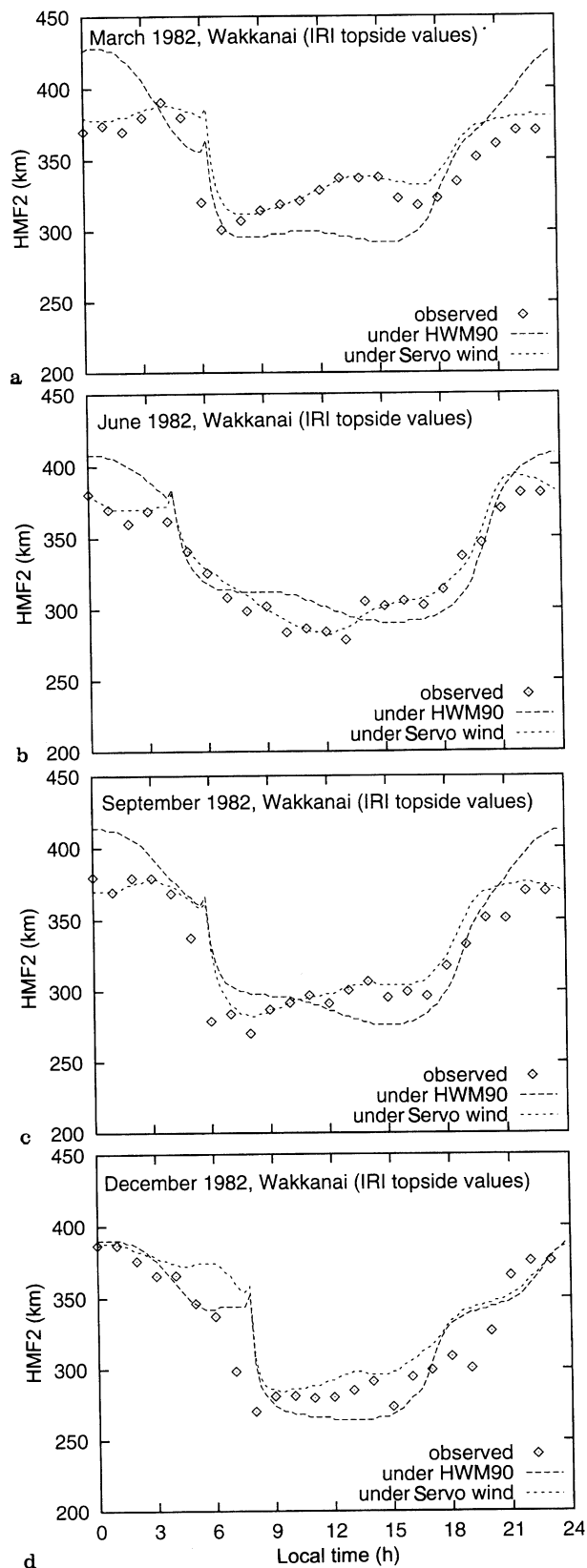


Fig. 1 a-d. Observed and simulated heights of the F₂ peak under different wind (or vertical drift) inputs over Wakkanai (high solar activity) for four seasons in 1982. Topside IRI values are used

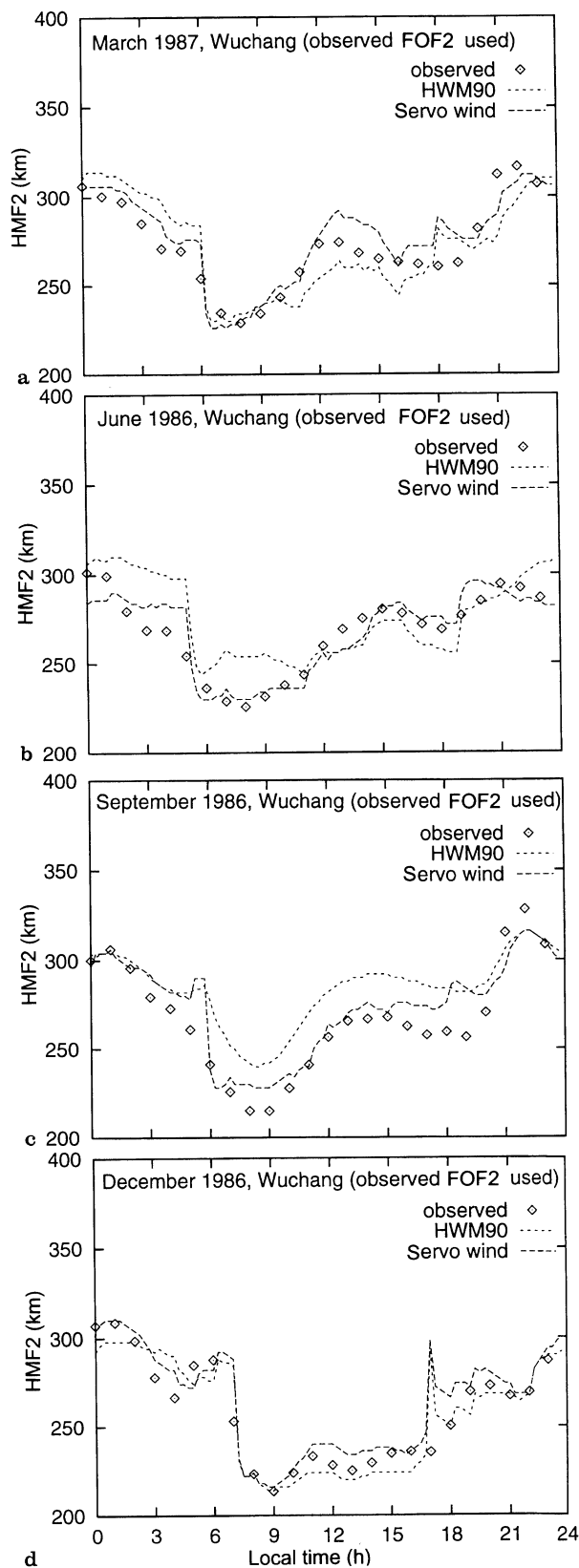


Fig. 2a-d. Observed and simulated heights of the F₂ peak under different wind (or vertical drift) inputs over Wuchang (low solar activity) for four seasons between 1986–1987. Observed *foF₂* is used to modify the initial topside values

diurnal fluctuation, “noise” and “jumps” seem inevitable. In addition, as our present model uses a constant time step of 15 min, which appears inadequate for sunrise and sunset periods.

In general, it can be found that the consistency between simulated hmF_2 and that observed varies with the wind (or vertical drift) term used, as well as with the topside values and the geophysical conditions. In fact, in the case of Wuchang (lower solar activity), better correlation occurs when the observed foF_2 is used, whilst, in the case of Wakkanai (higher solar activity), the agreement tends to be better with the IRI topside condition only. However, it is clear for all the cases we have studied that the Servo-model-based vertical drifts can reproduce the peak height better than the HWM90 model. Generally, the departure does not exceed 20 km, except near sunrise and sunset and is much less in many cases, and no disagreement can be detected more obviously for the period between sunrise and pre-noon compared to other periods (except near sunrise and sunset). As mentioned earlier, our calculation with the HWM90 as input does not take into account the electric field. Whether this may seriously modify the conclusion here needs to be investigated further

3.2 Ionospheric profile and F_1 -ledge

Ionospheric profiles are obtained by simultaneously using foF_2 and hmF_2 , so that initial topside values can be modified and derived vertical drifts can be introduced. The results indicate (Fig. 3) that the ionospheric profile below the peak changes significantly with season and solar activity. For the summer of lower solar activity (Fig. 3a) the F_1 -ledge is well-developed, whilst it almost disappears in the winter of high solar activity (Fig. 3b). This change coincides with observations. The behavior of the ionospheric E– F_1 -region depends strongly on the neutral composition, ionizing fluxes and cross sections, etc. Buonsanto (1990) and Buonsanto *et al.* (1992) showed the importance of accurate values for composition and flux and suggested modifications to the MSIS86 and the EUV91 models in order to gain reasonable success in modeling the E– F_1 -region ionosphere. However, it seems that one cannot properly describe the ledge if the model only contains a photo-chemical scheme. Within the framework of the present model where O^+ transport is always taken into account, we discuss the importance of meta-stable ions of O^+ , i.e., $O^+(^2D)$ and $O^+(^2P)$ and the molecular ions transport induced by neutral wind in the formation of the F_1 -ledge. Photo-chemical scheme where the meta-stable $O^+(^2D)$ (see also Su and Huang, 1991) and $O^+(^2P)$ are considered tends to give an obvious ledge. Whilst, if we consider only the stable ionic species reaction and omit the meta-stable ions [i.e. meta-stable ions produced by the EUV irradiance are simply set to the $O^+(^4S)$ production], the ledge becomes poorly developed (Fig. 4a). Wind-induced transport for all ionizations (molecular ions included) may also modify the shape of the ledge (see also Taieb *et al.*, 1978). It can be seen from Fig. 4a that the ledge becomes more evident when molecular ion transport is considered, whether meta-stable ions are in-

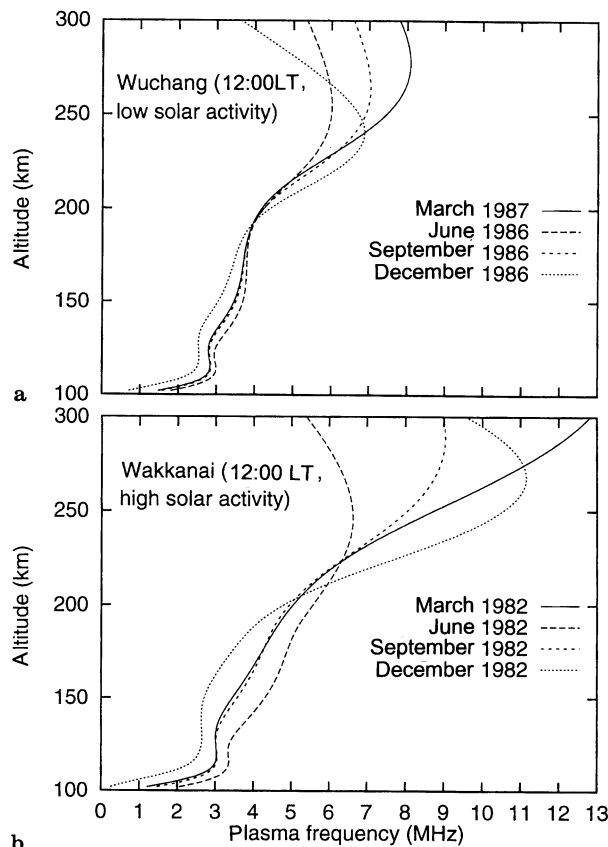


Fig. 3a, b. Simulated ionospheric profiles at 12:00 LT for four seasons under low and high solar activities with foF_2 and hmF_2 used simultaneously. **a** Wuchang (low solar activity), **b** Wakkanai (high solar activity)

involved or not in the photo-chemical scheme. So, when meta-stable ion and the wind-induced transport are all included, a well-developed ledge can be produced and more interestingly an F_1 – F_2 valley is formed (Fig. 4a). Using a different EUV model and different photoionization and photoabsorption cross sections (Torr and Torr, 1979) leads to the same conclusion (Fig. 4b). This means that meta-stable O^+ involved chemical reactions and wind-induced transport in the lower F_2 -region seem likely to form an obvious F_1 -ledge. Of course, changes of neutral composition and temperature may significantly affect the F_1 -layer, which we will discuss in another paper.

3.3 E–F valley structure

Valley depth and width are used to describe the E–F valley structure. The depth is defined here as the ratio of the bottom plasma frequency of the valley over the E-layer critical frequency foE . Results indicate (Fig. 5) that, in general, depth varies with local time and that this variability is not dependent on the time of year. Near noon the valley is deeper with a depth value of about 0.985 for lower solar activity (Wuchang) and 0.990 for higher solar activity (Wakkanai). The depth value seems quite

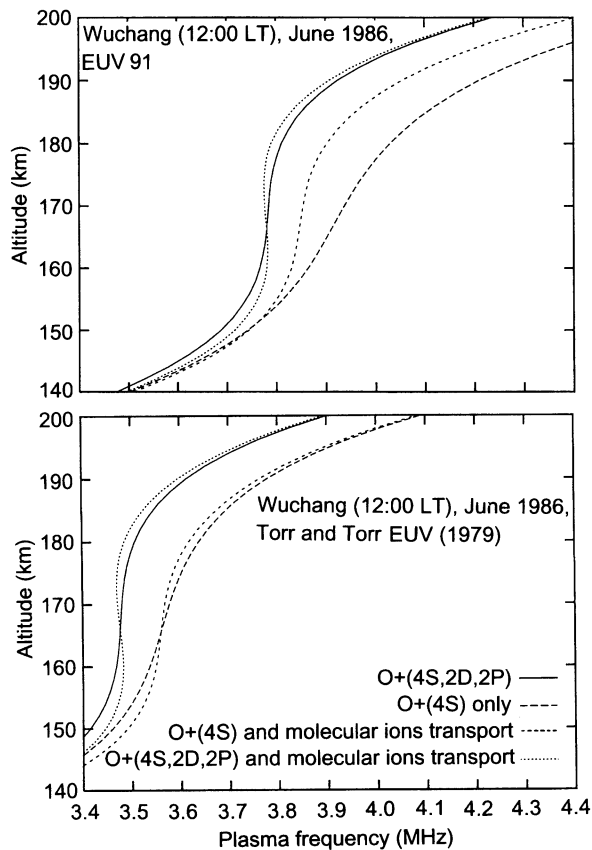


Fig. 4a, b. Effects of meta-stable ions and wind-induced transport on the formation of the F_1 -ledge for Wuchang at 12:00 LT, June 1986 (wind-induced O^+ drift is always included). **a** under the EUV91 model; **b** under the tabular model of Torr and Torr (1979)

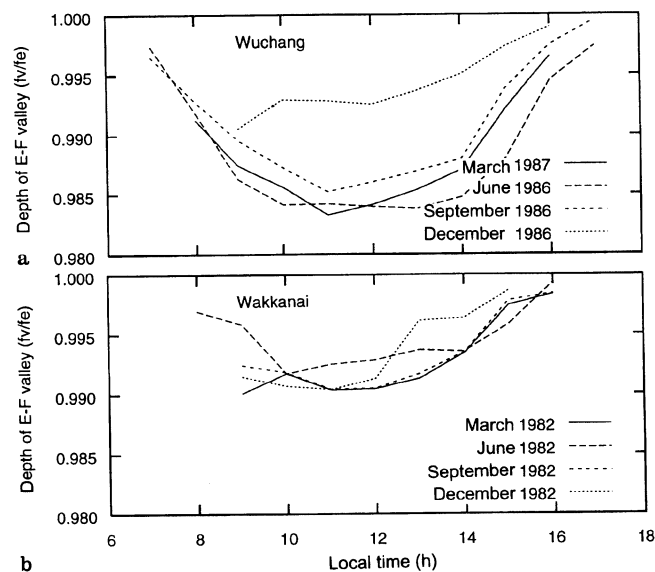


Fig. 5a, b. Ionospheric E-F valley depth for **a** Wuchang (low solar activity), **b** Wakkanai (high solar activity)

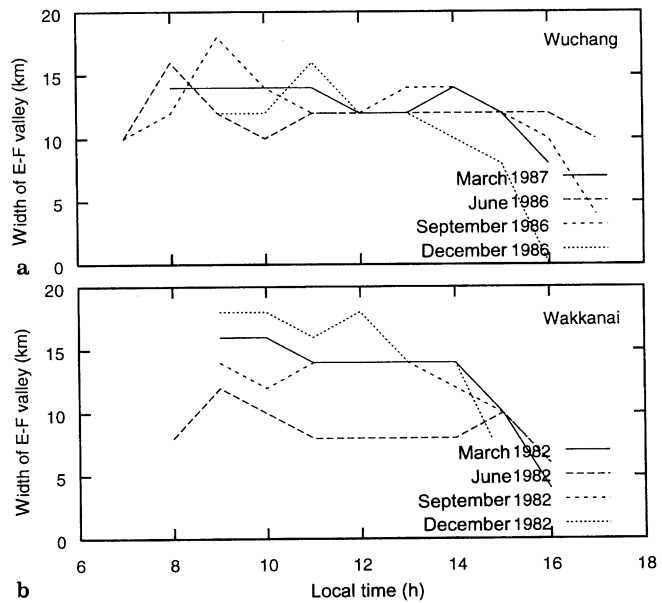


Fig. 6a, b. Ionospheric E-F valley width **a** Wuchang (low solar activity), **b** Wakkanai (high solar activity)

small. The valley width is the distance between the two altitudes with the same electron density as the E-layer peak. Although valley width changes very little near noon (10–14 LT), it does vary for other periods (Fig. 6). The lower solar activity corresponds to a width of 12 km or more whilst the width is a fraction greater at the higher solar activity. These results differ from those of the Titheridge model (1990), probably due to the adoption of different ionizing flux values; the latter used the tabulated results in 78 bands of Torr and Torr (1979). It should be noted that an inverse correction can be seen between the width and the depth. This is also similar to the observed results (Gulyeava, 1987).

4 Summary

A numerical model for the study of ionospheric profiles at mid-latitudes is developed. In this model, major ionospheric processes with an effect on O^+ , NO^+ , O_2^+ , N_2^+ are taken into account. In order to obtain more realistic ionospheric profiles, the simulated maximum density of the F_2 -layer is to be close to the observation and the height of the maximum density also approximately approaches the height deduced from the $M3000F_2$ factor. It is shown that, adopting vertical drifts derived from the Servo model can well reproduce the observed hmF_2 , while HWM90 generally could not. Thus, it seems reasonable to use such a method of fitting the key point on the ionospheric profile. Simulation further reveals the profile evolution. It is found that a fully developed F_1 -ledge occurs in the summer of lower solar activity. Also under certain conditions an F_1 – F_2 valley may exist, in which meta-stable oxygen ions play a significant role. Wind-induced transport for all ionic species also helps to produce the ledge and the valley. As for the E–F valley, it is deeper and a fraction narrower in lower solar activity than

in higher and also does not vary extensively during the daytime. The inverse correlation between the depth and width can be found.

Acknowledgements. The authors would like to thank the Goddard Space Flight Center for kindly providing the IRI90, MSIS86, HWM90 and EUV91 models. Thanks are also due to the Japanese Ministry of Post and Telecommunication for furnishing us with the ionosonde data. This work was supported by the National Natural Sciences Funds of China.

Editor-in-Chief, S. W. H. Cowley thanks G. Krichengast and J. Titheridge for their help in evaluating this paper.

References

- Bilitza, D.**, International Reference Ionosphere 1990, *National Space Science Data Center/World Data Center A for Rockets and Satellites*, 90–22, 1990.
- Buonsanto, M. J.**, A study of daytime E–F₁ region ionosphere at mid-latitudes, *J. Geophys. Res.*, **95**, 7735–7747, 1990.
- Buonsanto, M. J., J. E. Salah, K. L. Miller, W. L. Oliver, R. G. Burnside, and P. G. Richards**, Observations of neutral circulation at mid-latitude during the equinox transition study, *J. Geophys. Res.*, **94**, 987–997, 1989.
- Buonsanto, M. J., S. C. Solomon, and W. K. Tobiska**, Comparison of measured and modeled solar EUV flux and its effect on the E–F₁-region ionosphere, *J. Geophys. Res.*, **97**, 10,513–10,524, 1992.
- Dudeny, J. R.**, The accuracy of simple methods for determining the height of the maximum electron concentration of the F₂-layer from scaled ionospheric characteristics, *J. Atmos. Terr. Phys.*, **45**, 629, 1983.
- Gulyaeva, T. L.**, Progress in ionospheric informatics based on electron density analysis of ionograms, *Adv. Space Res.*, **7**(6), 39–48, 1987.
- Hedin, A. E.**, MSIS-86 thermospheric model, *J. Geophys. Res.*, **92**, 4649–4662, 1987.
- Hedin, A. E., M. A. Biondi, R. G. Burnside, G. Hernandez, R. M. Johnson, T. L. Kileen, C. Mazaudier, J. W. Meriwether, J. E. Salah, R. J. Sica, R. W. Smith, N. W. Spencer, V. B. Wickwar, and T. S. Virdi**, Revised globe model of thermospheric winds using satellite and ground-based observations, *J. Geophys. Res.*, **96**, 7657–7688, 1991.
- Henry, R. J. W., P. G. Burke, and A. L. Sinfailam**, Scattering of the electrons by C, N, O, N⁺, O⁺, and O⁺⁺, *Phys. Rev.*, **178**, 218–224, 1969.
- Huang, X.-Y., and J. Li**, Regional features of the ionosphere over China, in: *Advance in Chinese Solar-Terrestrial Physics*, Ed. Hu, W.-R., 173, Science Press, Beijing, 1992.
- Johnsen, R., and M. A. Biondi**, Laboratory measurements of the O⁺(²D) + N₂ and O⁺(²D) + O₂ reaction rate coefficients and their ionospheric implications, *Geophys. Res. Lett.*, **7**, 410–413, 1980.
- Kirchengast, G., R. Leitinger, and K. Schlegel**, A high-resolution model for the ionospheric F-region at mid- and high-latitude sites, *Ann. Geophysicae*, **10**, 577–596, 1992.
- Lindinger, W., F. C. Fehsenfeld, A. L. Schmeltekopf, and E. E. Ferguson**, Temperature dependence of some ionospheric ion-neutral reactions from 300–900 K, *J. Geophys. Res.*, **79**, 4753–4756, 1974.
- McFarland, M., D. L. Albritton, F. C. Fehsenfeld, E. E. Ferguson and A. L. Schmeltekopf**, Energy dependence and branching ratio of the N₂⁺ + O reaction, *J. Geophys. Res.*, **79**, 2925–2926, 1974.
- Mehr, F. J., and M. A. Biondi**, Electron temperature dependence of recombination O₂⁺ and N₂⁺ ions with electrons, *Phys. Rev.*, **181**, 264–271, 1969.
- Rishbeth, H., S. Ganguly and J. C. G. Walker**, Field-aligned and field-perpendicular velocities in the ionospheric F₂-layer, *J. Atmos. Terr. Phys.*, **40**, 767–784, 1978.
- Seaton, M. J., and D. E. Osterbrock**, Relative [O II] intensities in gaseous nebulae, *Astrophys. J.*, **125**, 66–83, 1957.
- St. Maurice, J. P., and D. G. Torr**, Nonthermal rate coefficients in the ionosphere: the reactions of O⁺ with N₂, O₂ and NO, *J. Geophys. Res.*, **83**, 969–977, 1978.
- Rees, M. H.** *Physics and Chemistry of the Upper Atmosphere*, Cambridge University Press, New York, 1989.
- Rusch, D. W., D. G. Torr, P. B. Hays, and J. C. G. Walker**, The O II (7319–7330 Å) dayglow, *J. Geophys. Res.*, **82**, 719–722, 1977.
- Sica, R. J., R. W. Schunk, and P. J. Wilkinson**, A study of the undisturbed mid-latitude ionosphere using simultaneous multiple-site ionosonde measurements during the Sundial-86 Campaign, *J. Geophys. Res.*, **95**, 8271–8279, 1990.
- Su, Y.-Z., and X.-Y. Huang**, Structure and variations of the ionospheric valley between F₁- and F₂-regions (in Chinese), *ACTA Geophys. Sin.*, **34**, 139–146, 1991.
- Taieb, C. G., Scialon, and G. Kockart**, A dynamical effect in the ionosphere F₁-region, *Planet. Space Sci.*, **26**, 1007–1016, 1978.
- Titheridge, J. E.**, Aeronomical calculations of valley size in the ionosphere, *Adv. Space Res.*, **10**(8), 21–24, 1990.
- Titheridge, J. E.**, Atmospheric winds calculated from diurnal changes in the mid-latitude ionosphere, *J. Atmos. Terr. Phys.*, **55**, 1637–1659, 1993.
- Tobiska, K.**, Revised solar extreme ultraviolet flux model, *J. Atmos. Terr. Phys.*, **53**, 1005–1018, 1991.
- Torr, D. R., and M. R. Torr**, Chemistry of the thermosphere and ionosphere, *J. Atmos. Terr. Phys.*, **41**, 797–839, 1979.
- Torr, D. R., and M. R. Torr**, Determination of the thermal rate coefficient, products, and branching ratios for the reaction of O⁺(²D) with N₂, *J. Geophys. Res.*, **85**, 783–787, 1980.
- Torr, D. R., and M. R. Torr**, The role of metastable species in the thermosphere, *Rev. Geophys. Space Phys.*, **20**, 91–144, 1982.
- Torr, D. R., M. R. Torr, J. C. G. Walker, A. O. Nier, L. H. Brace, and H. C. Britton**, Recombination of O₂⁺ in the ionosphere, *J. Atmos. Terr. Phys.*, **81**, 5578–5580, 1976.
- Walls, F. L., and G. H. Dunn**, Measurement of total cross sections for electron recombination with NO⁺ and O₂⁺ using ion storage techniques, *J. Geophys. Res.*, **79**, 1911–1915, 1974.
- Zhang, S.-R., X.-Y. Huang, Y.-Z. Su, and S. M. Radicella**, A physical model for one-dimension and time-dependent ionosphere. Part I. Description of the model, *Ann. Geofis.*, **36**(5–6), 105–110, 1993.